Multi-wavelength signals of dark matter at the Galactic center

Piero Ullio
SISSA & INFN (Trieste)

Based on: M. Regis & P.U., PRD 78 (2008) 043505, arXiv:0802.0234

TeV Particle Astrophysics IV, Beijing, September 24, 2008

The GC is an extraordinary site from different points of view. It hosts a ***supermassive black hole***, $M_{BH} \sim 3 \cdot 10^6\ M_\odot$, with position consistent with the compact radio source Sgr A*:

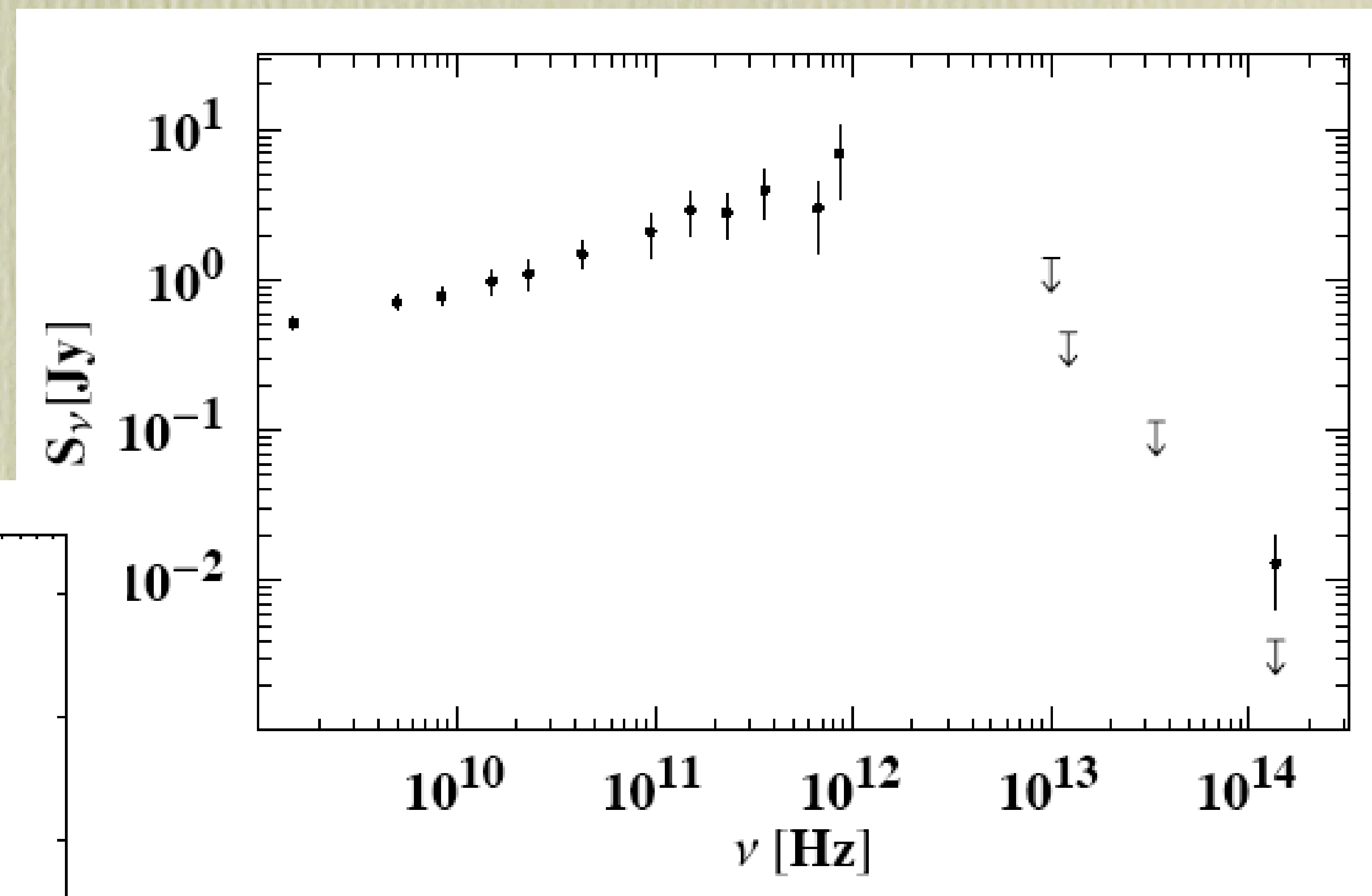

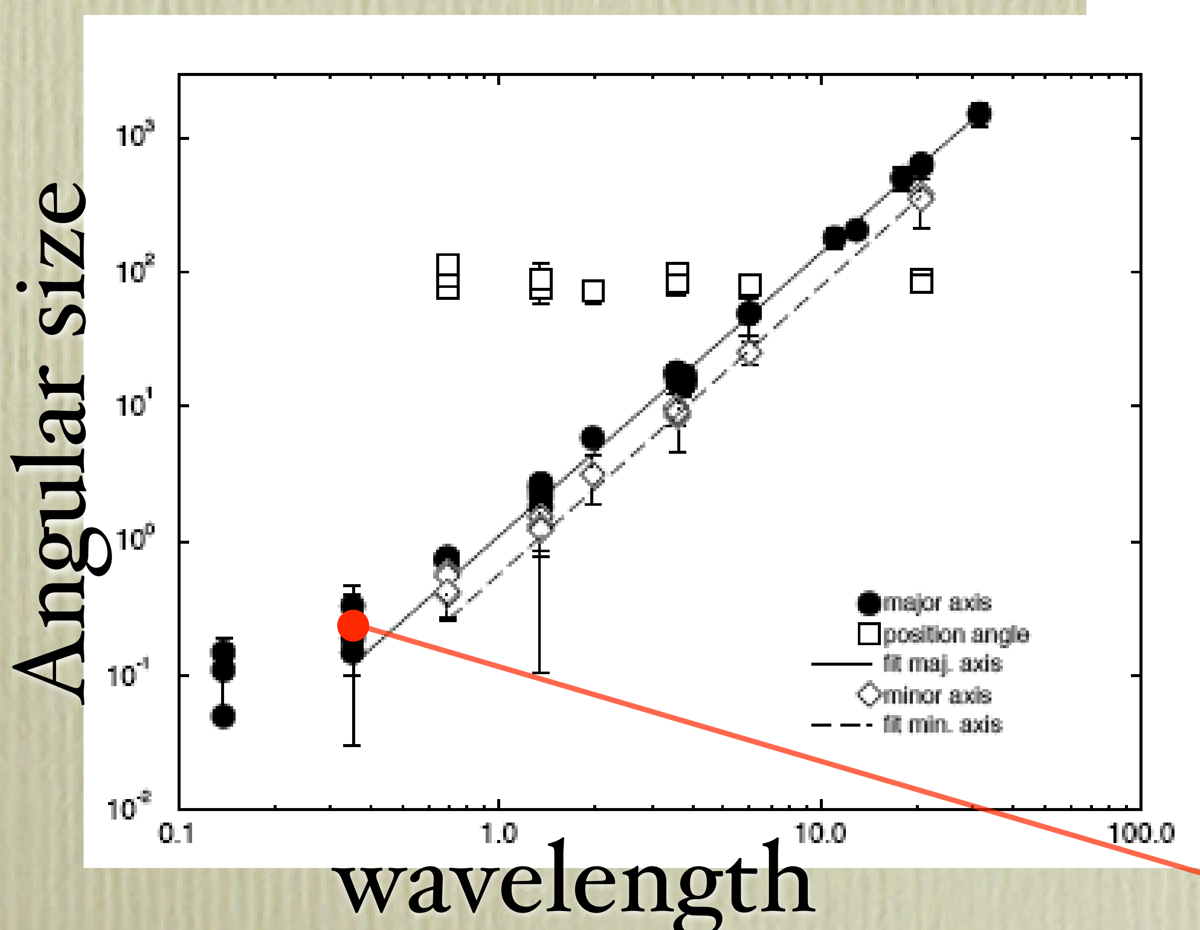

data re-binning by Melia & Falcke, 2001

0.18±0.02 mas, ~ 1 AU, ~ 12 RS, Shen et al., 2005

X-ray & γ-ray counterparts of Sgr A* have been (relatively) recently detected:

HESS discovery of a central source on top of a Galactic center ridge:

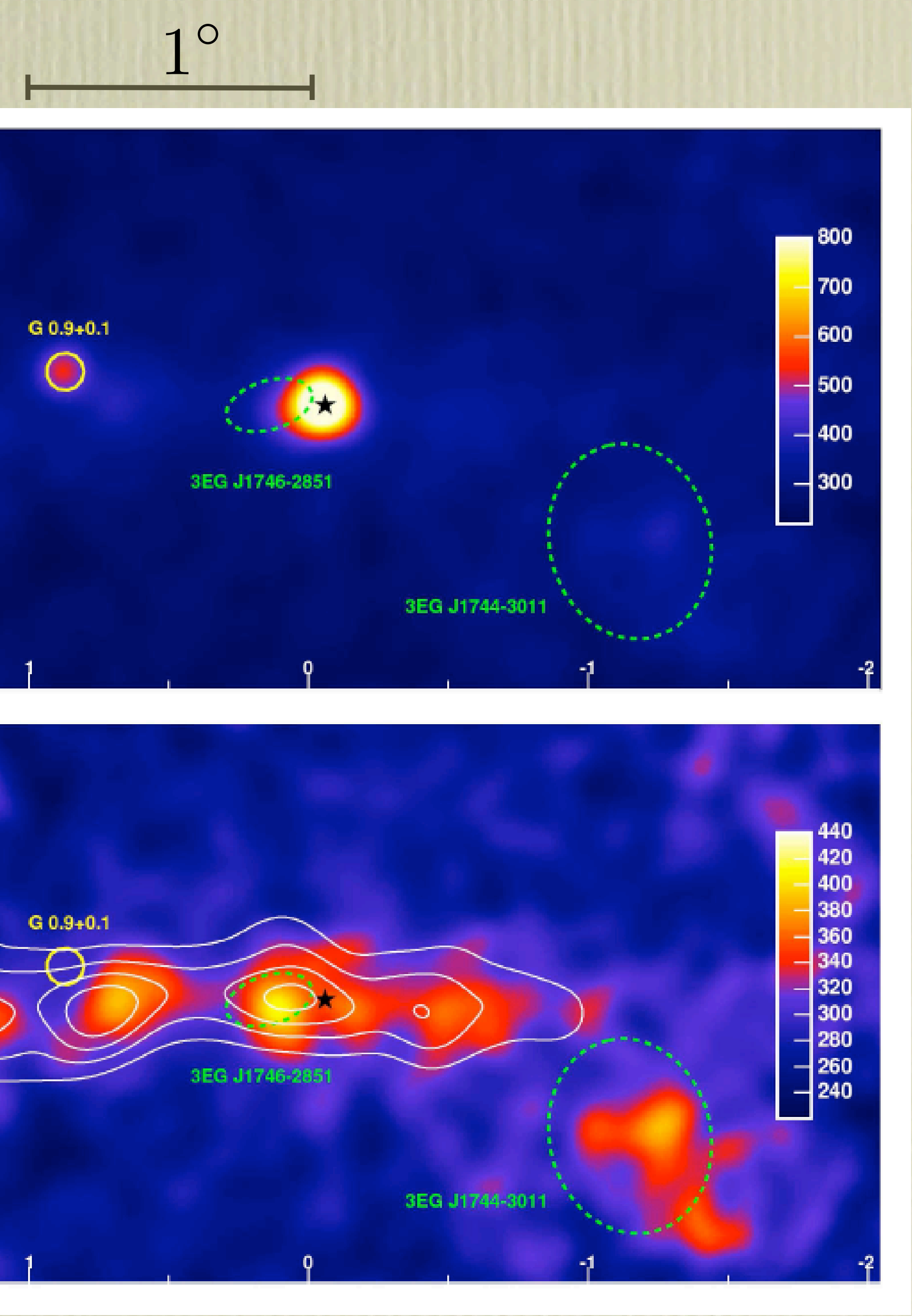

Aharonian et al., 2006

X-ray & γ-ray counterparts of Sgr A* have been (relatively) recently detected:

HESS discovery of a central source on top of a Galactic center ridge:

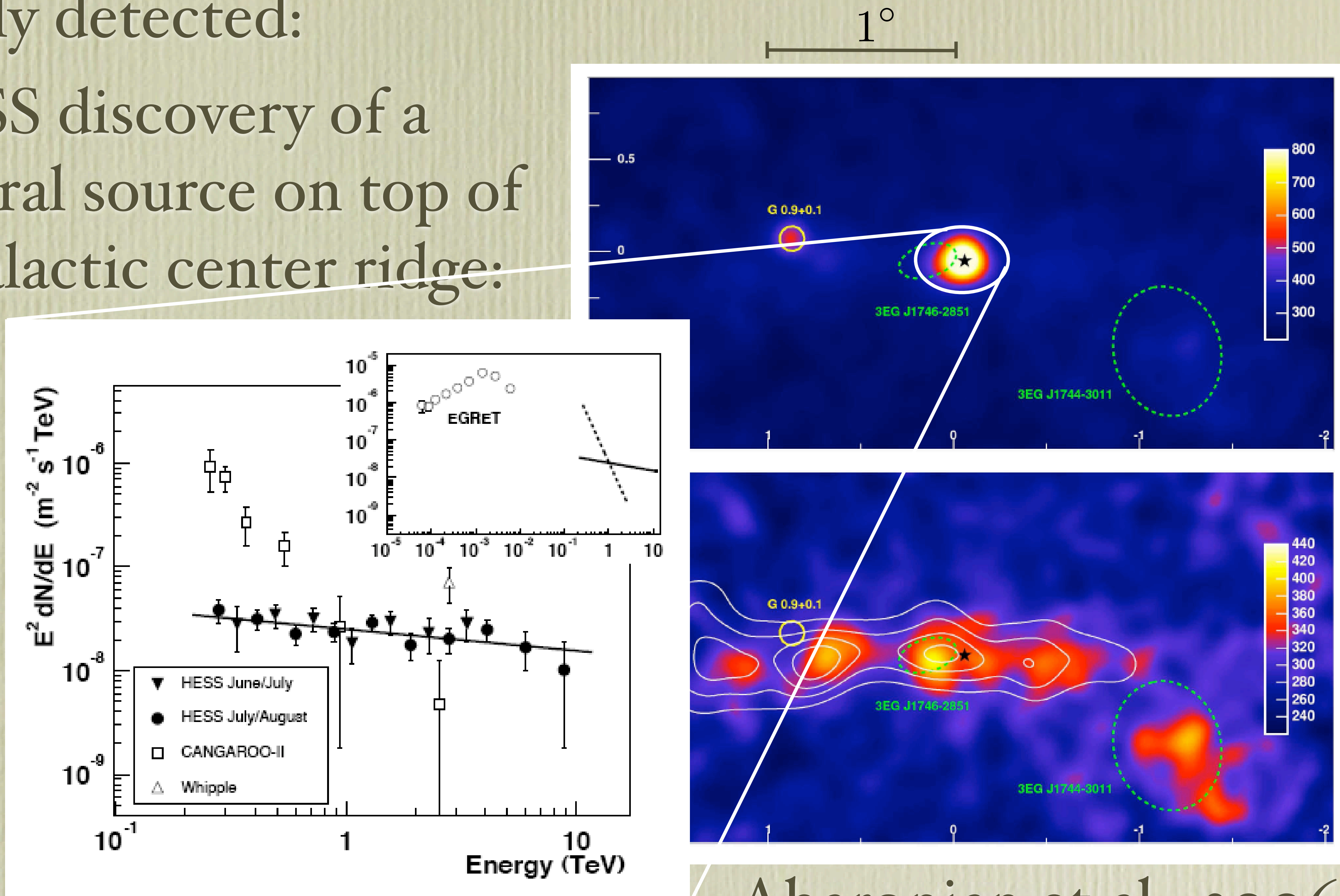

160 GeV → 20 – 30 TeV

Aharonian et al., 2006

Analogously, CHANDRA found diffuse emission + a central (< 0.5 arcsec) central source

Multi-wavelength seed of Sgr A* :

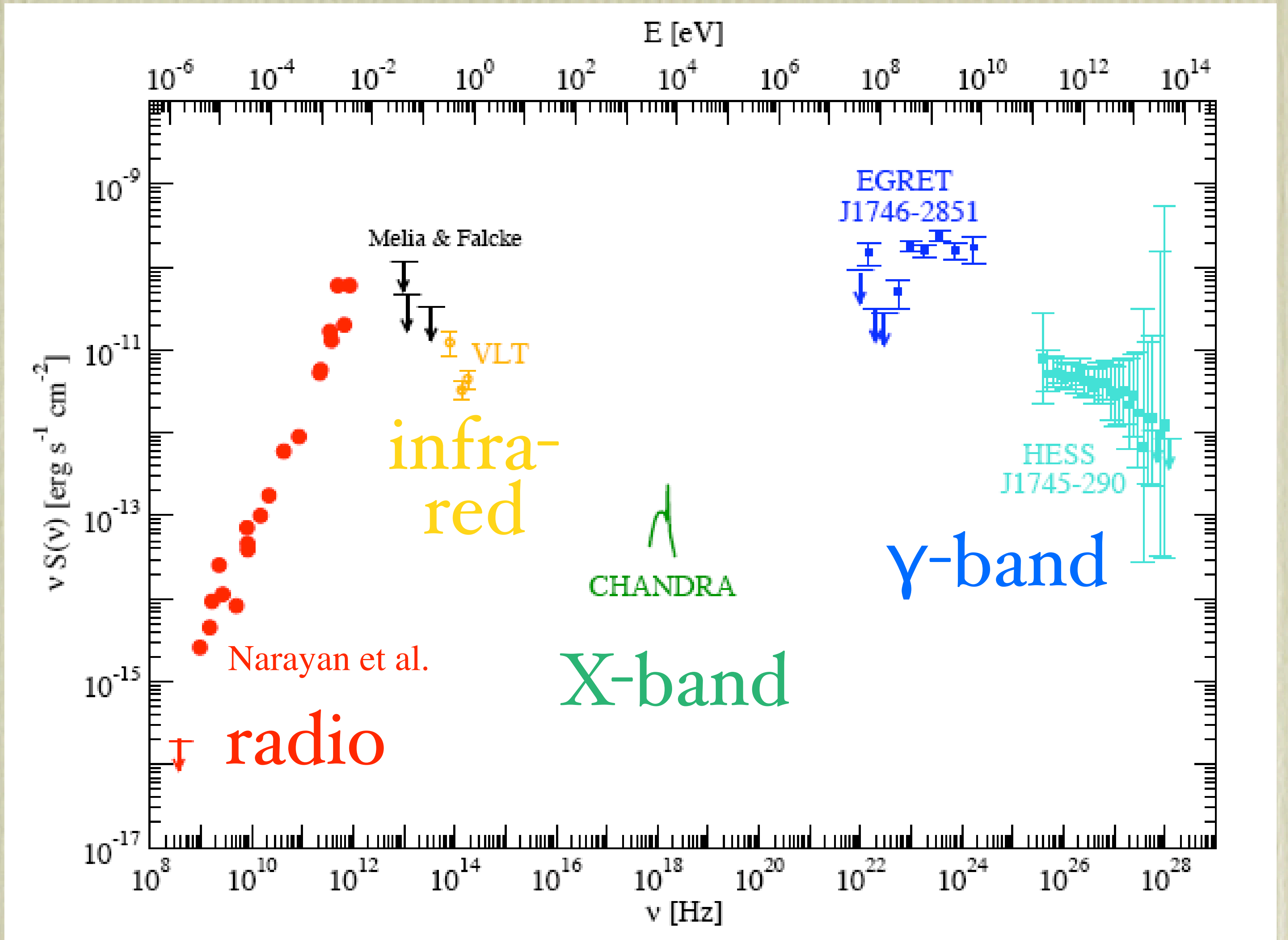

An unusual BH source, with low luminosity over the whole spectrum, at such a level that it is plausible for an exotic component, e.g. WIMP component, may be relevant!

Multi-wavelength signals from WIMP annihilations

WIMP CDM in DM halos:

$$\chi\,\chi$$

$$\downarrow \quad (\sigma v)_{T=0} \sim \langle \sigma v \rangle_{T=T_f}$$

and this matching:

$$\Omega_\chi h^2 \simeq \frac{3 \cdot 10^{-27} \mathrm{cm}^{-3} \mathrm{s}^{-1}}{\langle \sigma_A v \rangle_{T=T_f}}$$

1-loop states

$$\mathrm{SM}_1\ \mathrm{SM}_2$$

$$\boxed{\gamma\gamma \quad \gamma X^0}$$

(ϒ-lines)

$$\Downarrow$$

hadronization and/or decay

$$\overbrace{\ldots \quad \pi^0 \quad \pi^\pm}\ \longrightarrow e^\pm + \ldots$$

$$\pi^0 \downarrow 2\gamma$$

(ϒs with continuum spectrum)

ambient backgrounds and fields

- Synchrotron
- Inv. Compton
- Bremstrahlung
- Coulomb
- Ionization

- radio
- IR
- X-rays
- ϒs

WIMP source function:

$$Q_i(E,r) = (\sigma v)_0 \sum_f B_f \, \frac{dY_i^f}{dE}(E)\, \mathcal{N}_{\rm pairs}(r)$$

total rate

branching ratios

yield spectra

density of WIMP pairs

For a smooth DM distribution, i.e. no ignoring substructures:

$$\mathcal{N}_{\rm pairs}(r) = \frac{[\rho(r)]^2}{2\, M_\chi^2}$$

What is the halo density profile $\rho(r)$ for the GC region?

take a NFW profile, i.e. $\rho \propto 1/r$ at $r \to 0$ (a profile with a large core gives no WIMP signal at all wavelength!)

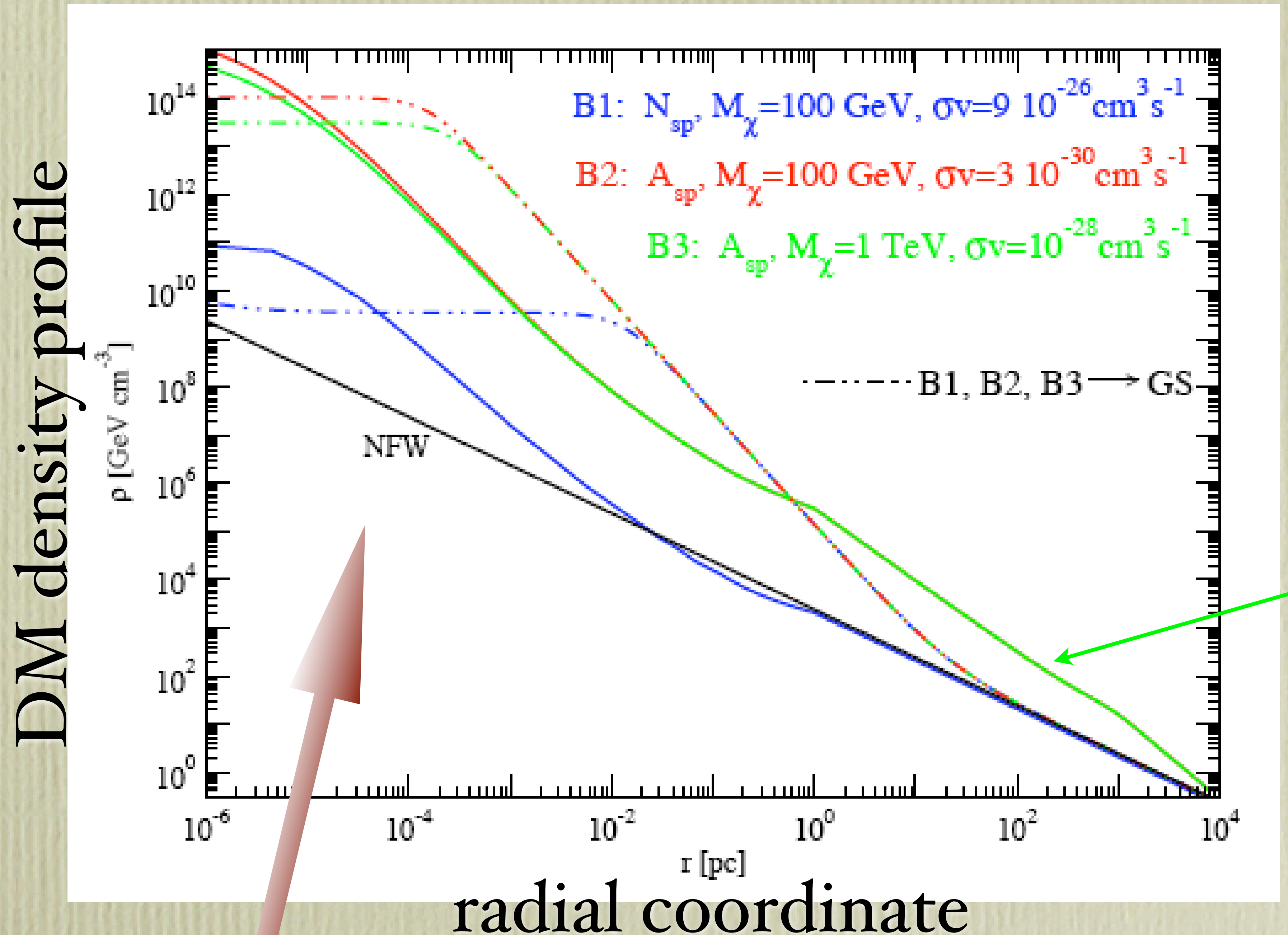

$1/r^{1.5}$ from adiabatic settling of stellar bulge

the adiabatic growth of the BH generates a DM "spike" (Gondolo & Silk, 1999); WIMP annihilations and scattering from stars included here (Bertone & Merritt, 2005)

What about photon and electron/positron yields?
Except for components from radiative emission or prompt decays, they are twin processes:

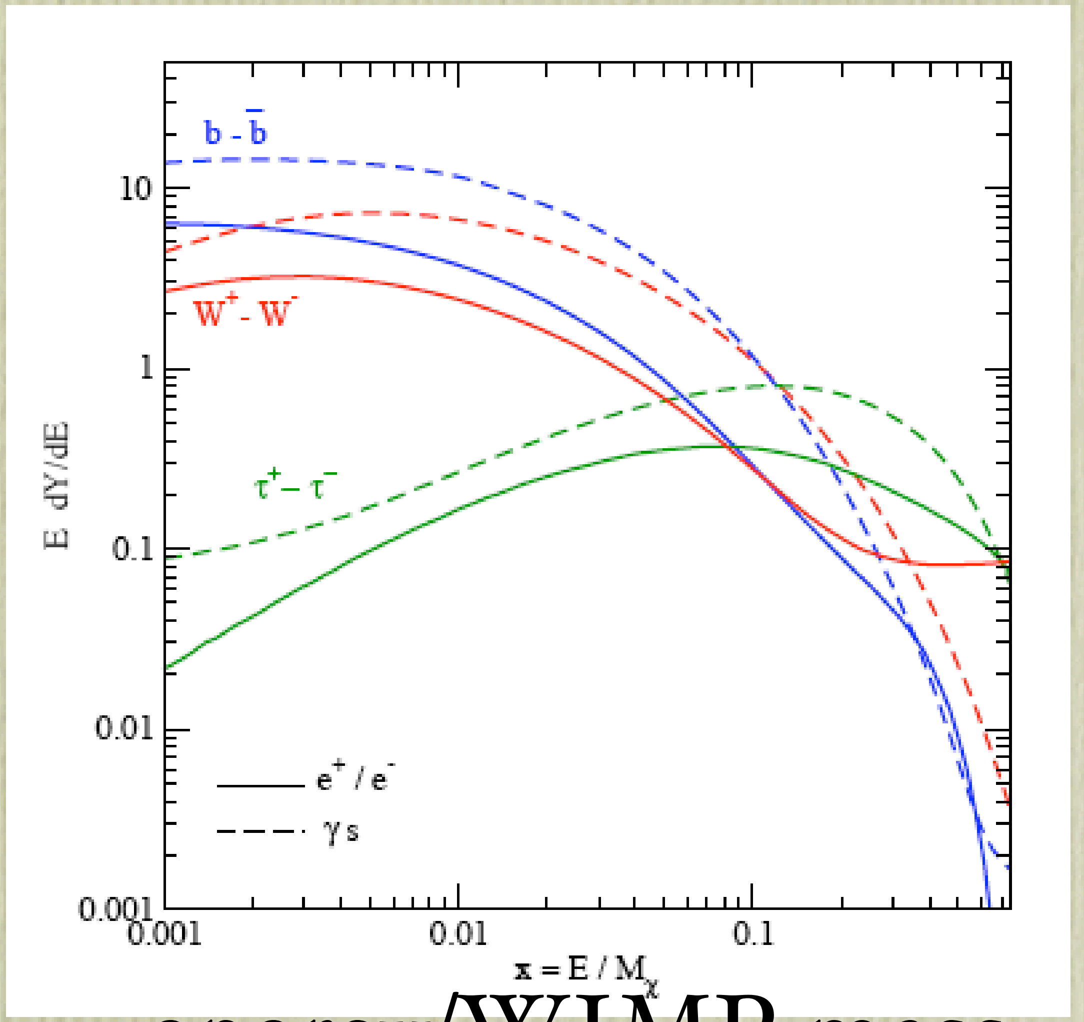

$$\frac{dY^f_{e^\pm}}{dE}(E)$$ from $\pi^\pm$ decays

(solid lines)

$$\frac{dY^f_{\gamma}}{dE}(E)$$ from π^0 decays

(dashed lines)

energy/WIMP mass

Whether you take a soft (e.g., $b - \bar{b}$) or hard (e.g.,$\tau^- - \tau^+$) the relative multiplicity is essentially constant!
Not necessary to focus on a specific WIMP model.

Predictions for radiative processes need a few steps:

i) compute equilibrium $e^- - e^+$ distribution functions:

$$\boxed{-\frac{1}{r^2}\frac{\partial}{\partial r}\left[D\frac{\partial}{\partial r}(r^2 f)\right]} + \boxed{v\frac{\partial f}{\partial r} - \frac{1}{3r^2}\frac{\partial}{\partial r}(r^2 v)\, p\frac{\partial f}{\partial p}} + \boxed{\frac{1}{p^2}\frac{\partial}{\partial p}(\dot{p}p^2 f)} = \frac{Q_e(r,E)}{4\pi\, p^2}\frac{dE}{dp}$$

spatial diffusion, negligible for GC

advection due to plasma inflow onto the BH

$$v(r) = -c\sqrt{\frac{R_{BH}}{r}}$$

radiative losses, mostly synchrotron emission in the large magnetic field in the GC region

see, e.g., Strong, Moskalenko & Ptuskin, 2007

ii) compute emissivities:

$$j_i(\nu, r) = 2\int_{m_e}^{M_\chi} dE\, P_i(r, E, \nu)\, n_e(r, E)\ ,$$

iii) compute intensities:

$$\frac{dI_i(\nu, s, \tilde{\theta})}{ds} = -\alpha(\nu, s, \tilde{\theta})\, I_i(\nu, s, \tilde{\theta}) + \frac{j_i(\nu, s, \tilde{\theta})}{4\pi}$$

Instructive shortcut: synchrotron emission and loss usually dominate. Assume synchrotron only and go to the monochromatic limit:

$$\nu \sim 0.29\,\nu_c \quad \text{with} \quad \nu_c = \frac{3}{4\,\pi}\,\frac{c\,e}{(m_e c^2)^3}\,B(r)\,E_p^2$$

i.e. for a given observed frequency and given peak energy in the radiating distribution, a matching value for $B(r)$ is needed.

Model the accretion flow and derive a sketch for the radial profile of the magnetic field:

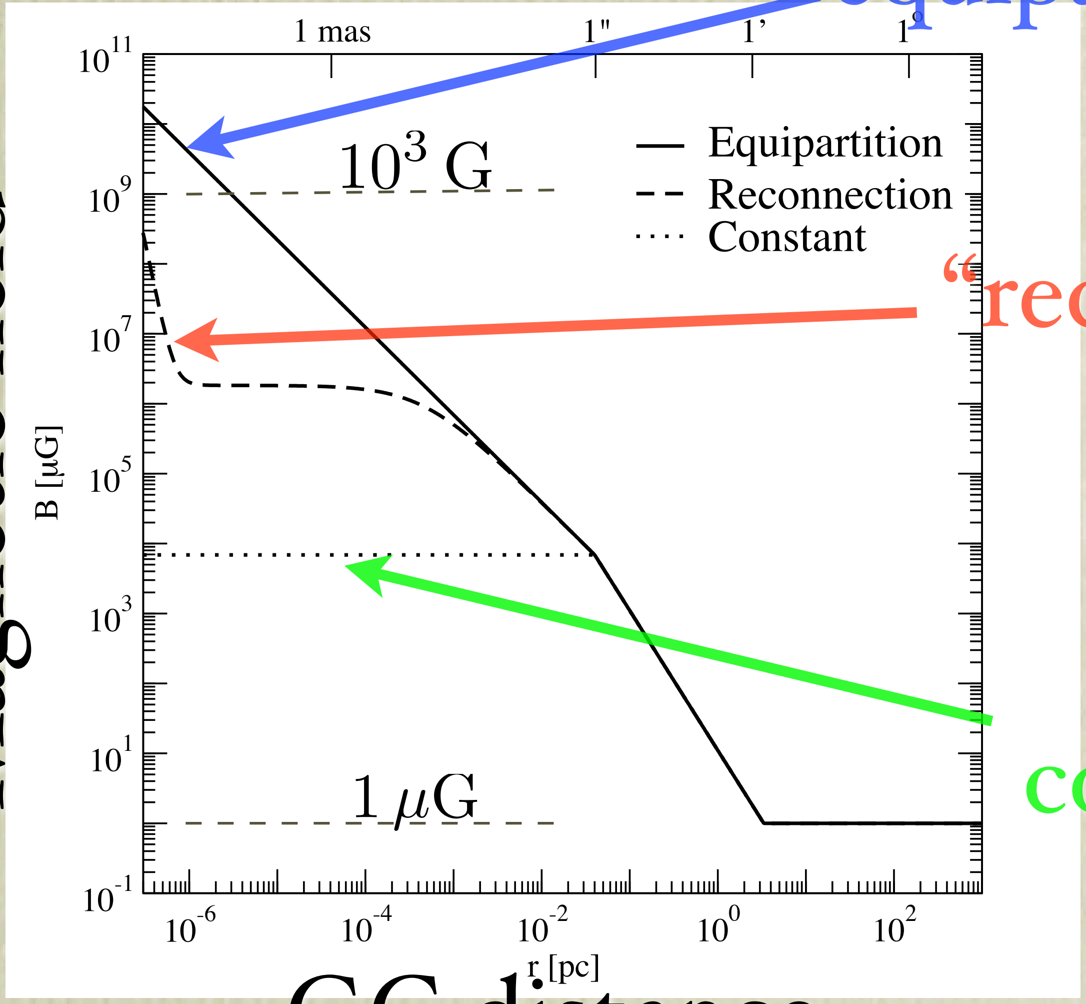

equipartition

"reconnection"

most conservative

Magnetic field

GC distance

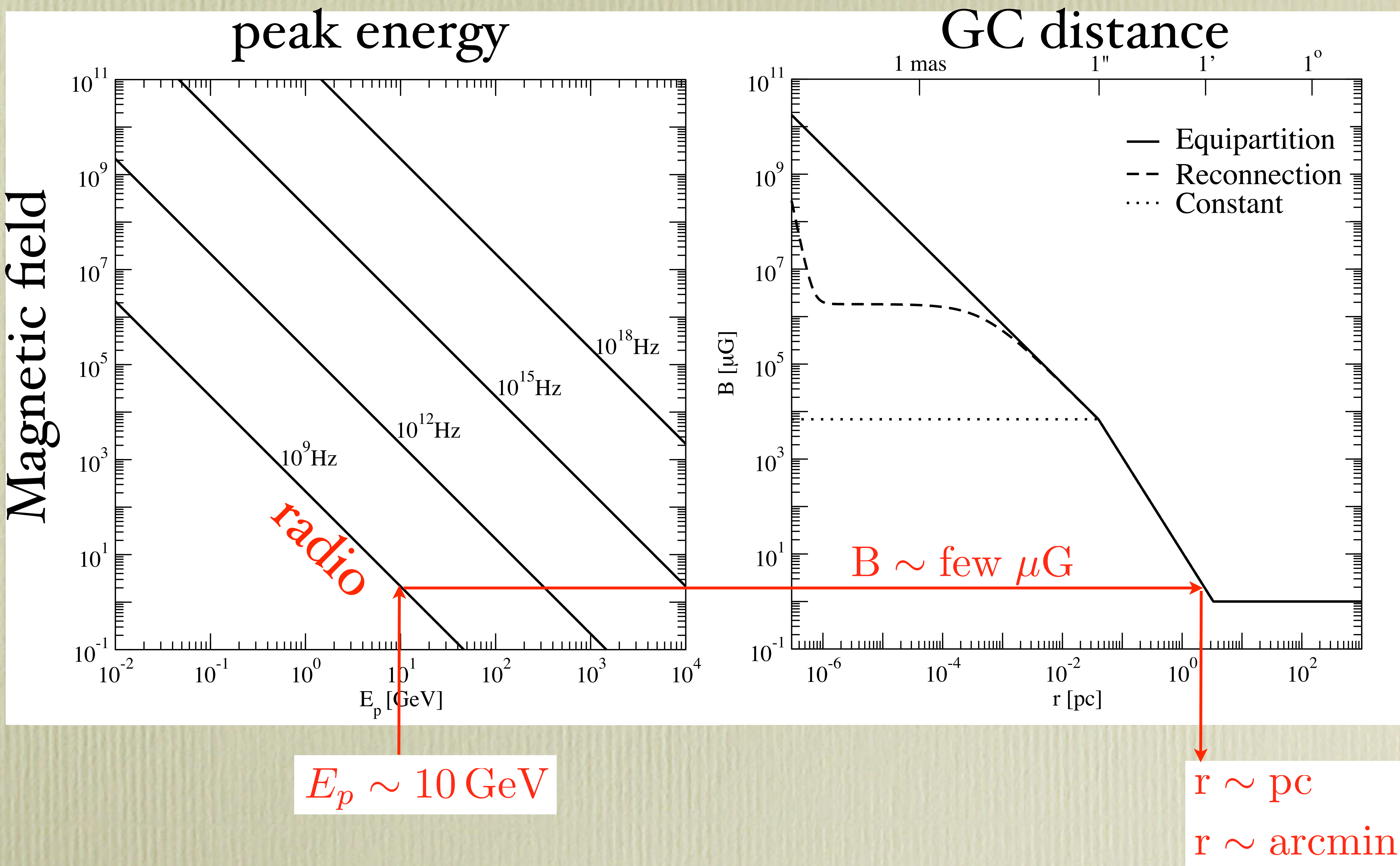

E.g., WIMP $M_\chi \sim 100\,\mathrm{GeV}$

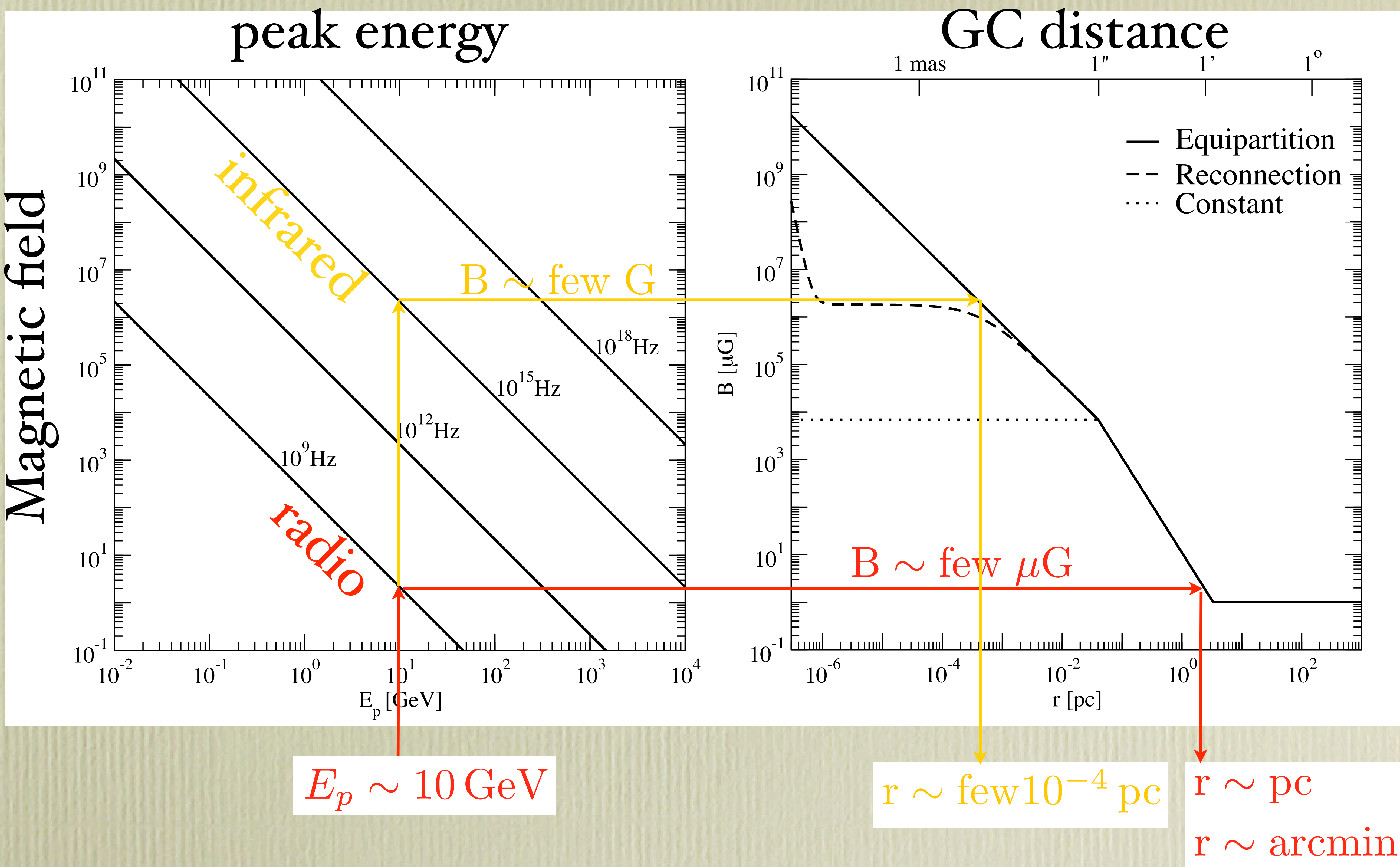

E.g., WIMP $M_\chi \sim 100\,\mathrm{GeV}$

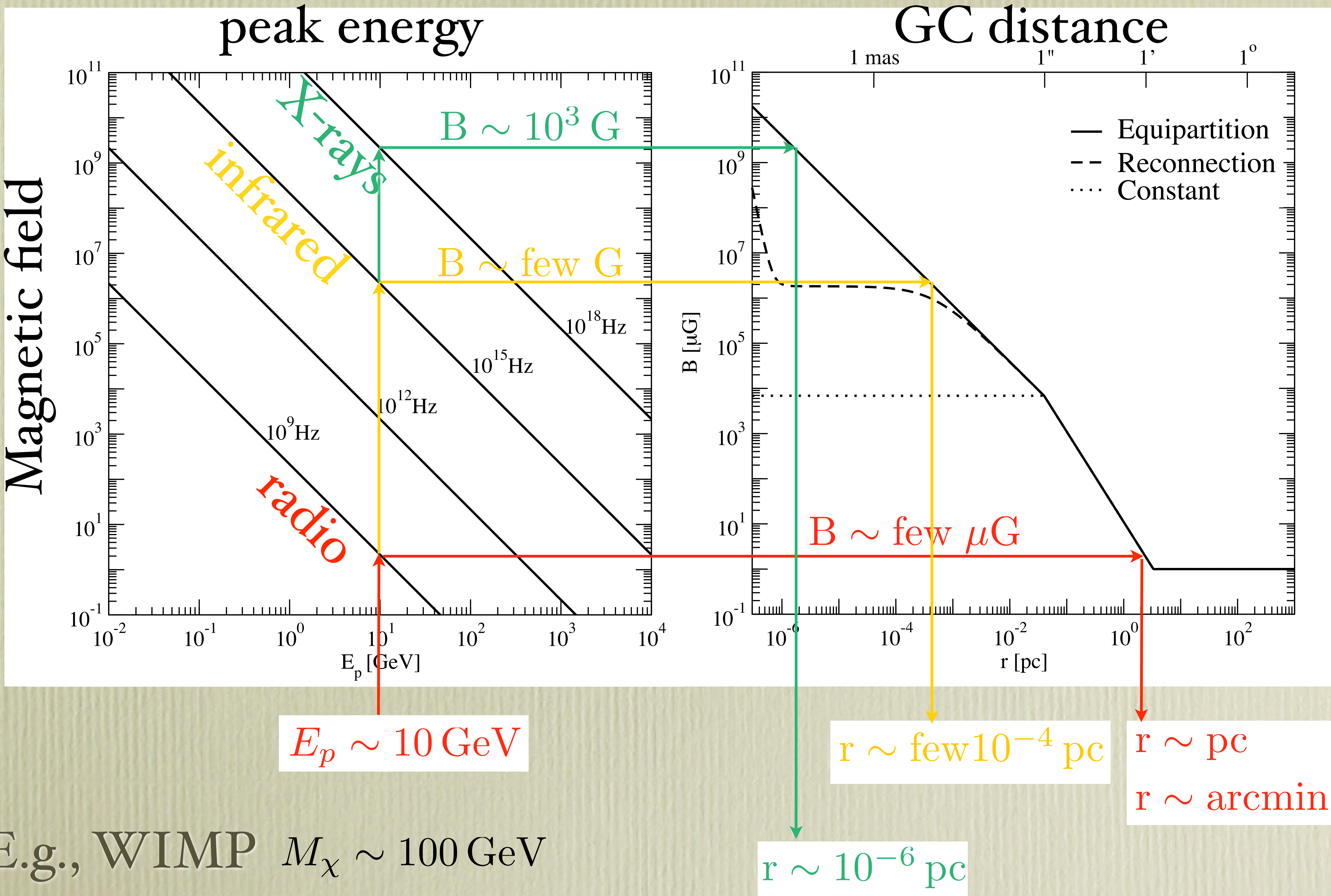

E.g., WIMP $M_\chi \sim 100\,\mathrm{GeV}$

Conclusion I: the X-ray emission may come from the very central region only, and depend crucially on B and WIMP mass, radio-emission spreads out to a larger region and are more model independent.

Take the approximate total radio luminosity:

$$\nu L_\nu^{syn} = \frac{9\sqrt{3}}{4}\frac{\sigma v}{M_\chi^2}\int dr\, r^2 \rho(r)^2 E_p\, Y_e(E_p)$$

with $Y_e(E_p)$ the integrated yield and $E_p = E_p(\nu, r)$.

Compare it the γ-ray total luminosity:

$$\nu L_\nu^\gamma = 2\pi \frac{\sigma v}{M_\chi^2}\int dr\, r^2 \rho(r)^2\, E^2 \frac{dN_\gamma}{dE}$$

Plug in numbers, typical ν and E, and find:

Conclusion II: the radio and gamma luminosities are at a comparable level.

When applying the full numerical treatment, we find that indeed the radio signal is wider than the width of the source (and hence of the γ-ray flux), while the X-ray signal is much smaller:

intrinsic

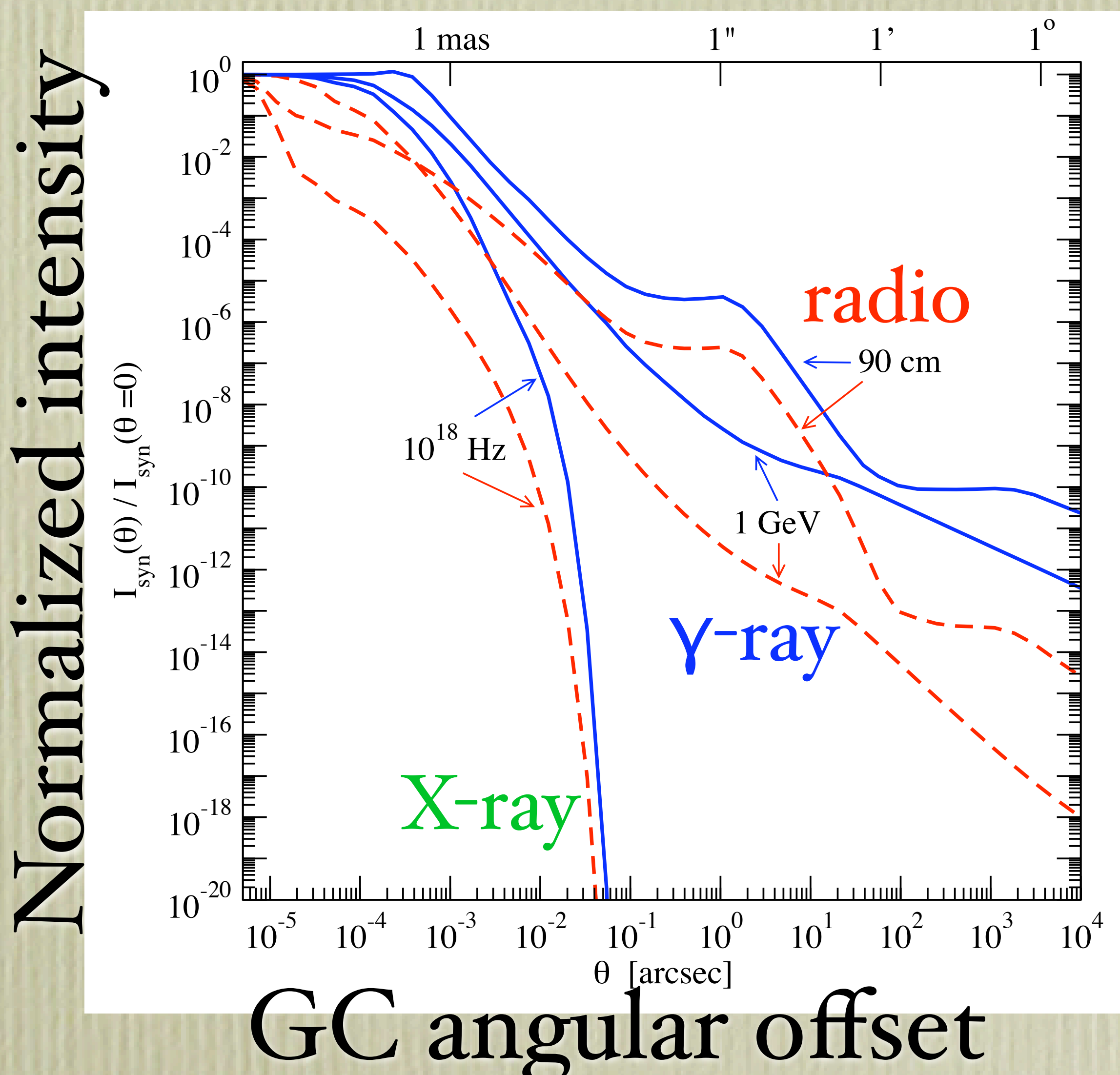

smoothed by gaussian detector response

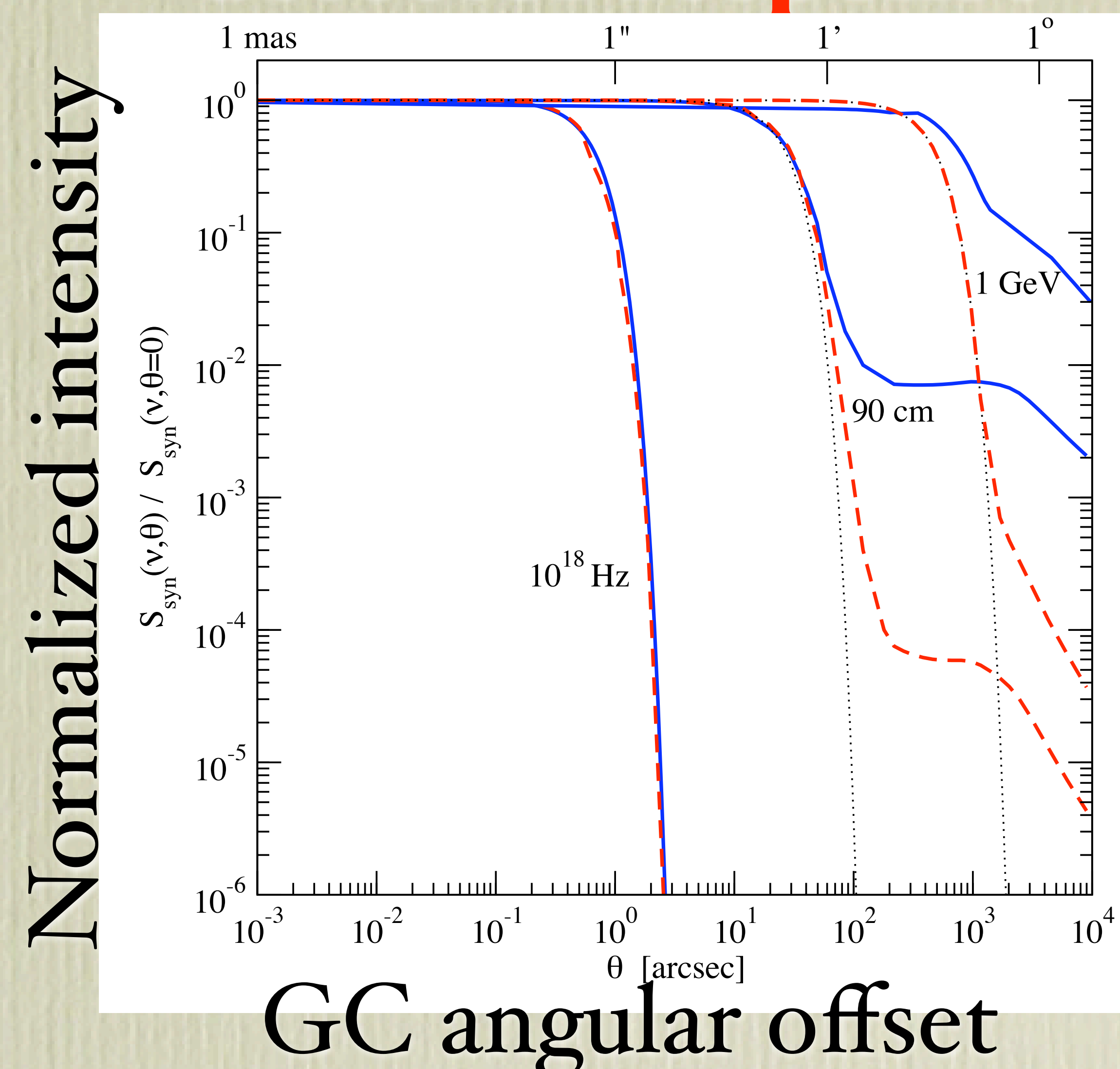

——— NFW + "Bertone & Merritt"

- - - - - $1/r^{1.5}$ + "Bertone & Merritt"

Synchrotron WIMP luminosities in the radio and infrared bands

integrated over entire source

Sgr A*

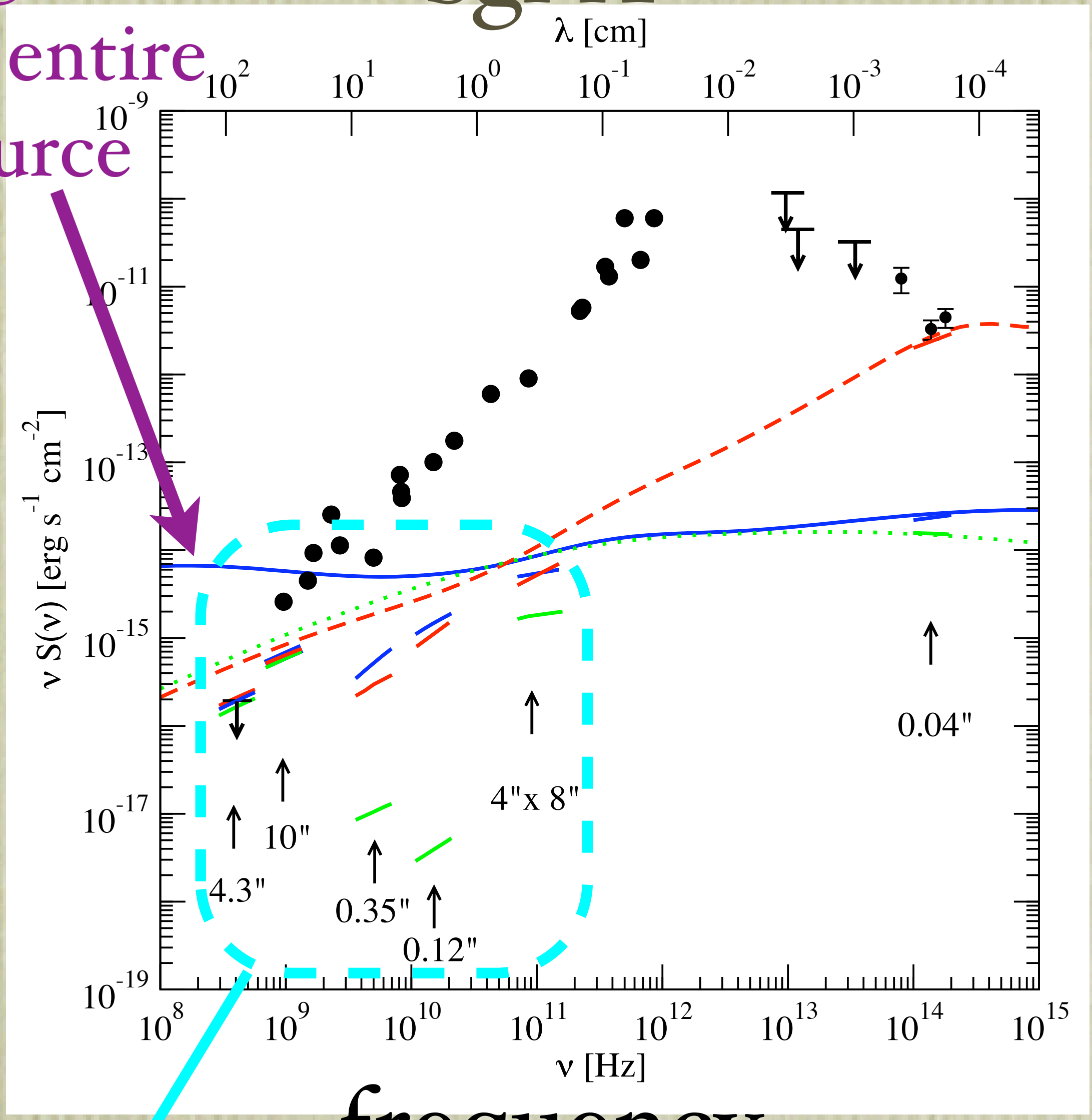

frequency

Sgr A + Sgr A*

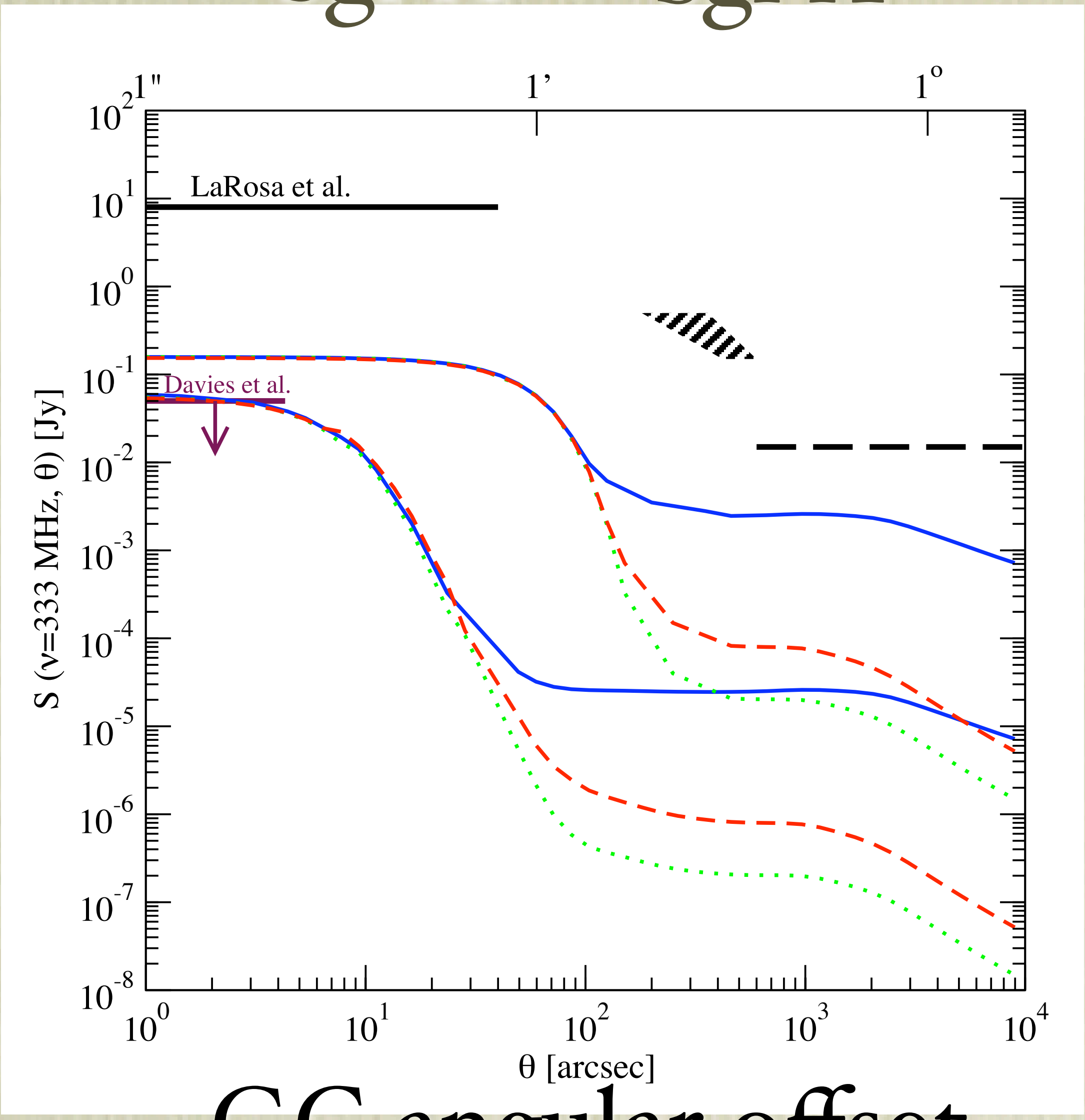

GC angular offset

simulating detector response

Note: the point-source approximation gives an overestimate of WIMP radio limits, future wide field radio surveys may be useful

Synchrotron WIMP luminosity in the X-ray band

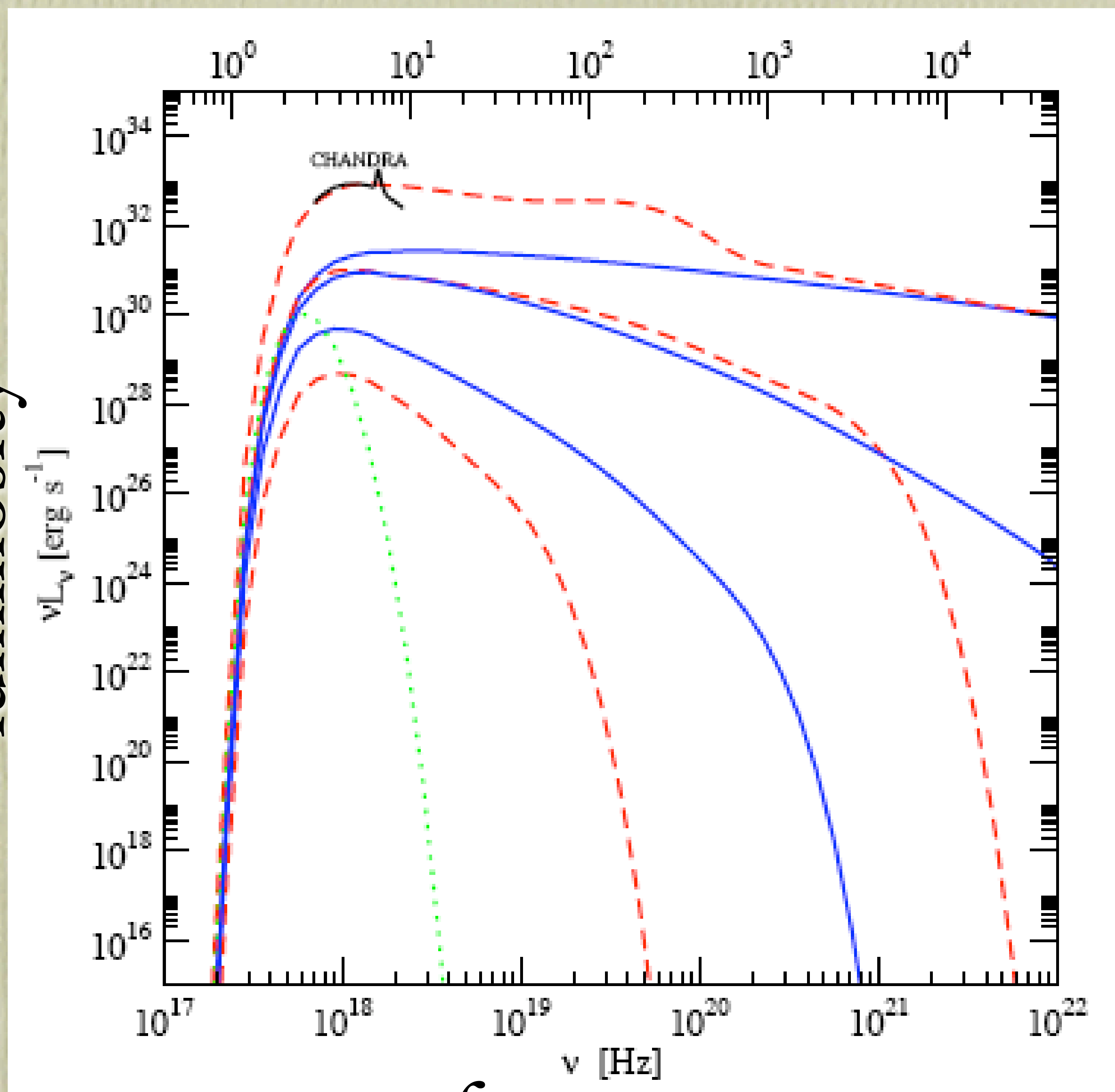

luminosity

frequency

equipartition B

reconnection B

constant B

1 TeV

↓

100 GeV

↓

10 GeV

Multi-wavelength limits in the plane WIMP mass – ann. cross-section

WIMP ann. cross-section

NFW + “Bertone & Merritt”

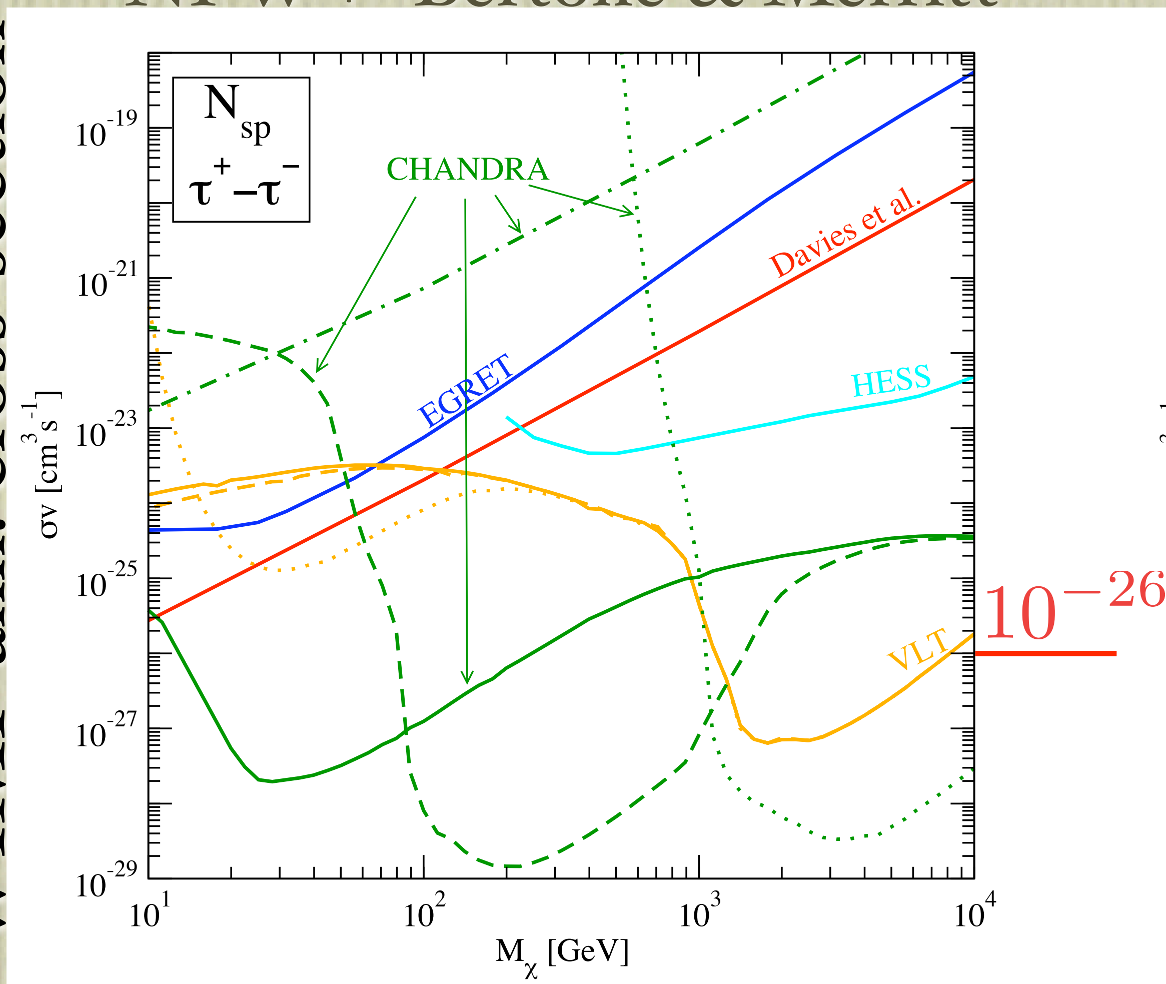

WIMP mass

$1/r^{1.5}$ + “Bertone & Merritt”

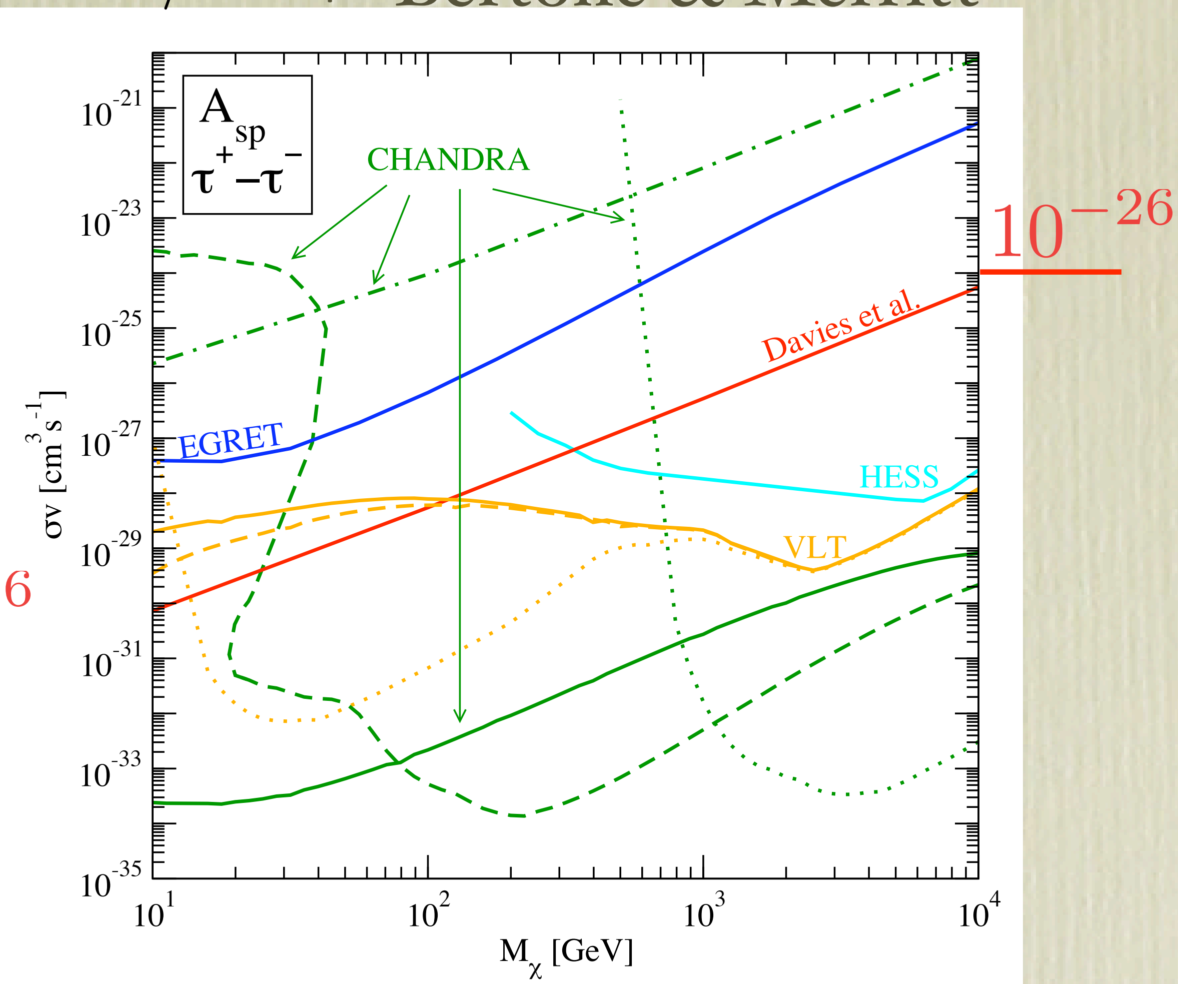

WIMP mass

HARD SPECTRA

——— equipartition B

– – – reconnection B

.... constant B

NOTE MISMATCH ON VERT. SCALE

Future perspectives: Fermi (GLAST), CTA & wide-field radio observations

HARD SPECTRA

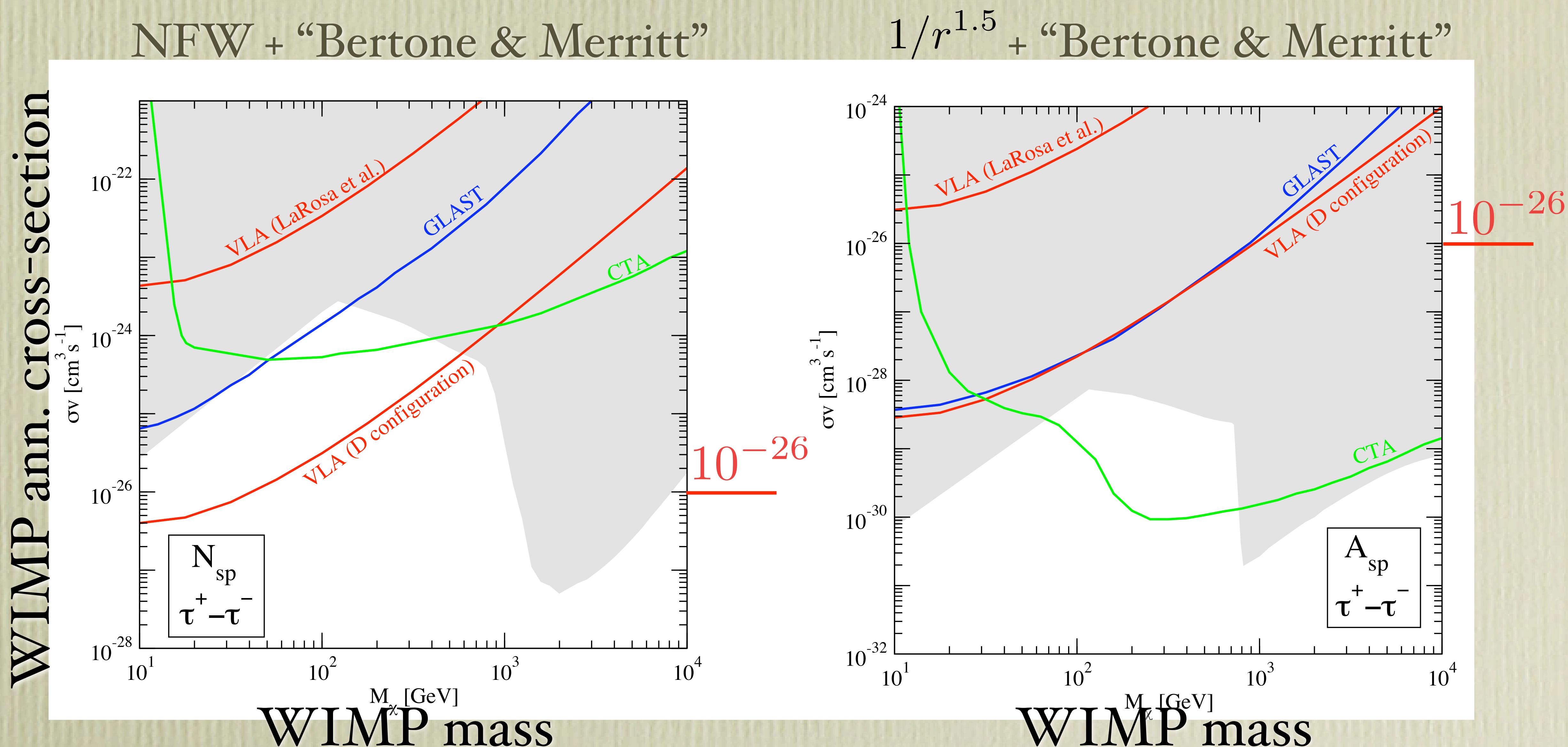

Moderate gain in γ-rays since there is a "background" source, better in radio in case of low background

NOTE MISMATCH ON VERT. SCALE

Multi-wavelength limits in the plane WIMP mass - ann. cross-section

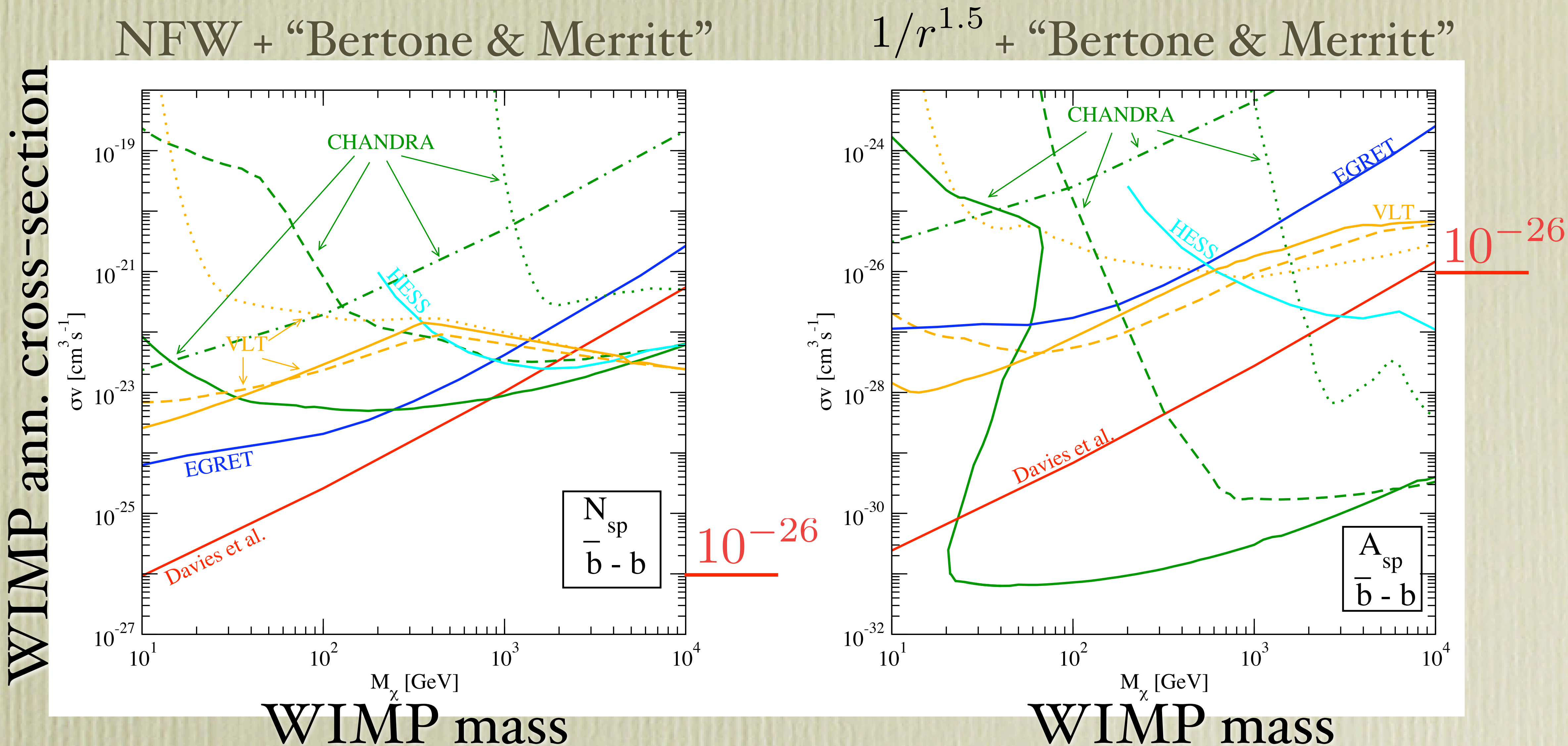

SOFT SPECTRA

equipartition B

reconnection B

constant B

NOTE MISMATCH ON VERT. SCALE

Future perspectives: Fermi (GLAST), CTA & wide-field radio observations

NFW + “Bertone & Merritt”

$1/r^{1.5}$ + “Bertone & Merritt”

WIMP ann. cross-section

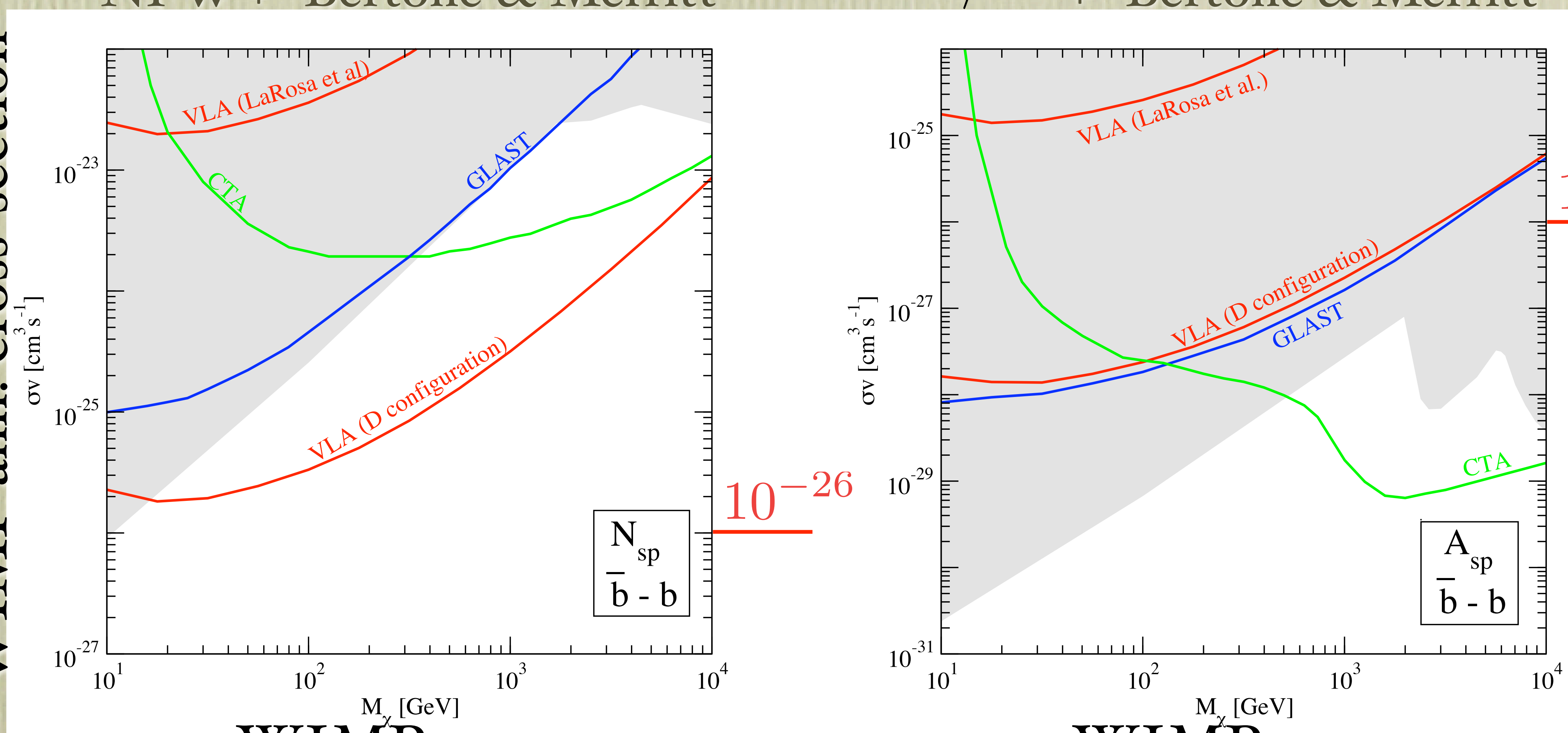

WIMP mass

WIMP mass

SOFT SPECTRA

NOTE MISMATCH ON VERT. SCALE

Conclusions

The multi-wavelength approach to WIMP indirect detection is very powerful when applied to the GC.

WIMP signals show definite patterns in source angular sizes and spectral features (unfortunately with no match to observations so far).

Constraints from currently available data pile up; datasets at all energy bands are relevant.

The gamma-ray band may not be the most promising to set stronger limits or possibly detect a WIMP DM component, as commonly assumed when neglecting the signals at other frequencies.